The Journal of Infectious Diseases

MAJOR ARTICLE

Germinal Center-Induced Immunity Is Correlated With Protection Against SARS-CoV-2 Reinfection But Not Lung Damage

Green Kim,[1,2,a] Dong Ho Kim,[3,a] Hanseul Oh,[1,a] Seongman Bae,[4] Jisoo Kwon,[4] Min-Jae Kim,[4] Eunyoung Lee,[5] Eun-Ha Hwang,[1,2] Hoyin Jung,[1] Bon-Sang Koo,[1] Seung Ho Baek,[1] Philyong Kang,[6] You Jung An,[1,] Jae-Hak Park,[7] Jong-Hwan Park,[2] Kwang-Soo Lyoo,[8] Choong-Min Ryu,[9] Sung-Han Kim,[4,b,] and Jung Joo Hong[1,10,b,]

[1]National Primate Research Centre, Korea Research Institute of Bioscience and Biotechnology, Cheongju, Chungcheongbuk, Republic of Korea, [2]Laboratory Animal Medicine, College of Veterinary Medicine, Chonnam National University, Gwangju, South Jeolla, Republic of Korea, [3]Department of Pediatrics, Korea Cancer Center Hospital, Seoul, Republic of Korea, [4]Department of Infectious Diseases, Asan Medical Center, University of Ulsan College of Medicine, Seoul, Republic of Korea, [5]Division of Infectious Diseases, Department of Internal Medicine, Korea Cancer Center Hospital, Seoul, Republic of Korea, [6]Futuristic Animal Resource Centre, Korea Research Institute of Bioscience and Biotechnology, Cheongju, Chungcheongbuk, Republic of Korea, [7]Department of Laboratory Animal Medicine, College of Veterinary Medicine, Seoul National University, Seoul, Republic of Korea, [8]Korea Zoonosis Research Institute, Chonbuk National University, Iksan, Republic of Korea, [9]Infectious Disease Research Centre, Korea Research Institute of Bioscience and Biotechnology, Daejeon, Republic of Korea, and [10]Bioscience, Korea University of Science & Technology (UST), Daejeon, Republic of Korea

Germinal centers (GCs) elicit protective humoral immunity through a combination of antibody-secreting cells and memory B cells, following pathogen invasion or vaccination. However, the possibility of a GC response inducing protective immunity against reinfection following severe acute respiratory syndrome coronavirus 2 (SARS-CoV-2) infection remains unknown. We found GC activity was consistent with seroconversion observed in recovered macaques and humans. Rechallenge with a different clade of virus resulted in significant reduction in replicating virus titers in respiratory tracts in macaques with high GC activity. However, diffuse alveolar damage and increased fibrotic tissue were observed in lungs of reinfected macaques. Our study highlights the importance of GCs developed during natural SARS-CoV-2 infection in managing viral loads in subsequent infections. However, their ability to alleviate lung damage remains to be determined. These results may improve understanding of SARS-CoV-2–induced immune responses, resulting in better coronavirus disease 2019 (COVID-19) diagnosis, treatment, and vaccine development.

Keywords. germinal center; SARS-CoV-2; viral reinfection; lung damage.

Germinal centers (GCs) in the secondary lymphoid tissues elicit protective humoral immunity following pathogen invasion and/or vaccination through a combination of antibody-secreting cells (ASCs) and memory B cells (MBCs) [1]. Within GCs, B cells interact with T follicular helper (TFH) cells, and antigen-presenting cells [2] undergo proliferation, isotype-switching, and affinity maturation through somatic hypermutation of the B-cell receptor. Following the initial GC reactions, antigen-specific immunoglobulin M (IgM) and switched immunoglobulins generated from GC-related ASCs and MBCs circulate in the blood. The GC activity persists after disease resolution and antigen disappearance; however, its level depends on the pathogen and severity of infection [3]. Typically, recovered patients acquire long-term immune memory and have antibodies for pathogen neutralization, in case of reinfection.

In coronavirus disease 2019 (COVID-19) caused by severe acute respiratory syndrome coronavirus 2 (SARS-CoV-2), the antibody kinetics and relationship between protective antibody levels and GC formation need elucidation. There is a possibility of reduced antibody durability upon GC formation [4, 5]; however, following COVID-19 symptoms, the rate of protective antibody formation is high in most recovered patients [6–9]. This indicates GC development and long-term immunity. Interestingly, there is a substantial decrease in GC B and TFH cell numbers and the absence of GCs in the lymphoid tissues of patients who succumb to COVID-19 [10]. SARS-CoV-2 infection might hamper the durability of antibody responses by disrupting the GC structure. However, the modulation of GC-associated protective immune responses following natural SARS-CoV-2 infection, particularly in recovered patients who experienced mild or moderate symptoms, has not been evaluated. It also remains unclear whether the generation of GCs following natural infection is beneficial in preventing disease progression, including viral replication and lung damage, during SARS-CoV-2 reexposure.

Received 20 June 2021; editorial decision 12 October 2021; accepted 14 October 2021; published online 20 November 2021.

aG. K., D. H. K., and H. O. contributed equally to this study.

[b]S. -H. K., and J. J. H. equally contributed to this study as senior authors.

Correspondence: Jung Joo Hong, DVM, PhD, National Primate Research Centre, Korea Research Institute of Bioscience and Biotechnology, 30 Yeongudanji-ro, Ochang-eup, Chengwon-gu, Cheongju, Chungcheongbuk, Republic of Korea (hong75@kribb.re.kr).

The Journal of Infectious Diseases® 2021;224:1861–72

https://doi.org/10.1093/infdis/jiab535

We used cynomolgus macaques to recapitulate COVID-19 in humans. The monkeys neither develop severe symptoms nor die from COVID-19 [11–13], and were therefore used for comprehensive quantitative and qualitative analyses of GC reactions induced by primary SARS-CoV-2 infection. We provide insights into the protective humoral immunity elicited by natural infection with SARS-CoV-2 and the potential success of a COVID-19 vaccine.

METHODS

Cells and Viruses

African green monkey kidney cell Vero (CCL-81; American Type Culture Collection) was maintained in Dulbecco's modified Eagle medium (Welgene Inc), supplemented with 10% fetal bovine serum (Gibco, Thermo Fisher Scientific) and 100 U/mL penicillin–streptomycin (Gibco).

SARS-CoV-2 virus (NCCP no. 43326 for the S clade [A, 19B] and NCCP no. 43345 for the GH clade [B.1, 20C]) was obtained from the National Culture Collection for Pathogens (Cheongju, Republic of Korea). The D614G mutation was identified in the spike proteins of the 2 strains.

Animal Studies

The cynomolgus macaques were anesthetized with a combination of ketamine sodium (10 mg/kg) and tiletamine/zolazepam (5 mg/kg) for viral challenges and swab and blood collection. Details of animal studies are presented in the Supplementary Methods.

Plaque Reduction Neutralization Test

The neutralization assay was conducted using the PRNT50 assay on Vero cells at approximately 95% confluence in 6-well tissue culture plates. Details of the procedure are presented in the Supplementary Methods.

Flow Cytometric Analyses of Macaque Blood, Spleen, and Lymph Node Cells

PBMCs and lymph node cells (LNs) were stained as previously described with slight modifications [14]. Details of the staining procedure are presented in the Supplementary Methods.

Histopathology and Immunofluorescence Staining

The lung and spleen of infected macaques were harvested at 3 or 21 days after S clade infection and at 3 days after GH clade infection, fixed with 4% paraformaldehyde, embedded in paraffin, and sectioned. The sectioned lung tissues were stained with hematoxylin and eosin, Masson's trichrome, or Sirius red. Immunofluorescence staining of the serial sections was performed using a previously described protocol with some modifications [15]. Details of the staining procedure are presented in the Supplementary Methods.

ELISA and Enzyme-Linked Immunospot (ELISPOT) Assay

Details of the enzyme-linked immunosorbent assay (ELISA) and enzyme-linked immunospot assay (ELISPOT) procedures are presented in the Supplementary Methods.

Anti-CD3 and Anti-CD28 Monoclonal Antibody Treatment

To induce the differentiation of COVID-19–specific MBCs, 96-well plates were coated with 1 μg/mL anti-CD3 antibody (clone OKT3; cat. no. 317302; BioLegend) or anti-CD3 antibody (clone SP34; cat. no. 557052; BD Bioscience) and left overnight. After washing with phosphate-buffered saline, the cells (500 000 cells/well) were cultured in complete Roswell Park Memorial Institute (RPMI) 1640 medium containing 1 μg/mL soluble anti-CD28 antibody (clone CD28.2; cat. no. 555725; BD Bioscience) at 37°C under 5% CO_2 for 4 days.

Analysis of Human Normal and Convalescent Plasma

From February 2020 to July 2020, we prospectively enrolled 13 patients with COVID-19 in the Asan Medical Center. Plasma samples from 12 healthy volunteers, collected before the COVID-19 outbreak, were used as the healthy controls during analysis. From April 2020 to August 2020, 8 patients in the Korea Cancer Center Hospital were diagnosed with COVID-19 using real-time reverse transcription polymerase chain reaction (RT-PCR). Plasma samples of the convalescent patients were collected 2–4 weeks after discharge and stored at −80°C until further analysis. Details of the procedure are presented in the Supplementary Methods.

Quantification and Statistical Analysis

Statistical analyses were performed using the 1-way ANOVA with Dunnett multiple comparisons test or Student unpaired *t* test using Prism version 8.4.2 (GraphPad Software, Inc). All results are expressed as mean ± standard error of the mean (SEM). Statistical significance was defined as $P < .05$.

Study Approval

All participants were informed of the nature of the study, and they provided written informed consent. The study protocol was approved by the institutional review board of the Asan Medical Center (study No. 2020-0299) and the Korea Cancer Center Hospital (IRB No. 2020-04-014-001). The clinical information on patients and healthy volunteers is listed in Supplementary Tables 1 and 2.

RESULTS

GC-Dependent Immunity in Convalescent Patients

Spike protein (S1 and S2)-specific IgG, IgM, and IgA were detected only in the convalescent patients with COVID-19 (Figure 1A). We assessed neutralizing activity (NA) using the 2-fold plasma dilution assay, with dilutions ranging from 1:40 to 1:1280. The SARS-CoV-2–specific NA was higher in convalescent patients with COVID-19 than in healthy individuals

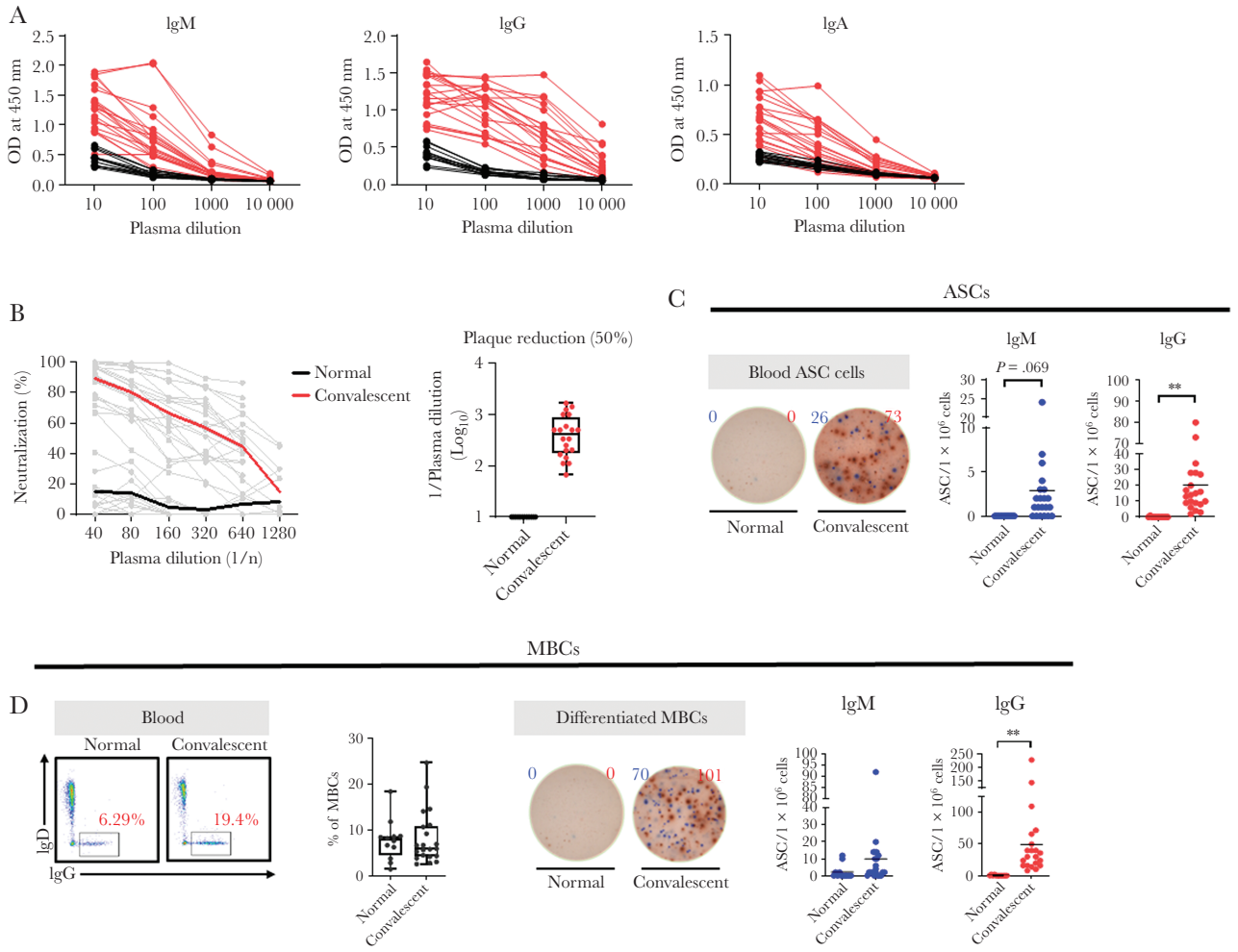

Figure 1. GC-dependent immunity in convalescent patients. *A*, SARS-CoV-2 spike protein (S1+S2)-specific IgM, IgG, and IgA responses: red and black data points/lines show the results for plasma from convalescent samples (n = 21) and healthy control samples (collected before the COVID-19 outbreak; n = 12), respectively. *B*, Neutralization is indicated according to plasma dilution at the indicated dpi. The SARS-CoV-2 plaque reduction was 50%. *C*, Representative ELISPOT data of SARS-CoV-2 spike protein (S1+S2)-specific IgM (blue) and IgG (red) ASCs in human PBMCs. Circles represent individual data and the line represents mean (unpaired Student *t* test; $^{**}P < .01$). Data are presented as mean ± SEM. *D*, Frequency of MBCs in PBMCs from healthy and convalescent samples. Representative ELISPOT data of SARS-CoV-2 spike protein (S1+S2)-specific IgM (blue) and IgG (red) ASCs differentiated from MBCs over 4 days using anti-CD3 and anti-CD28 monoclonal antibodies (1 μg/mL). Circles represent individual data and the line represents mean (unpaired Student *t* test; $^{**}P < .01$). Data are presented as mean ± SEM. Abbreviations: ASC, antibody-secreting cell; COVID-19, coronavirus disease 2019; dpi, days postinfection; ELISPOT, enzyme-linked immunospot; GC, germinal center; Ig, immunoglobulin; MBC, memory B cell; OD, optical density; PBMC, peripheral blood mononuclear cell; SARS-CoV-2, severe acute respiratory syndrome coronavirus 2.

(Figure 1B). The positive rate of IgM-secreting cells was 71.4% (15/21), which was significantly lower than the positive rate of circulating IgM-secreting (100%) and IgG-secreting cells (100%) (Figure 1C). MBCs with the potential to secrete IgGs specific for SARS-CoV-2 were significantly higher in convalescent patients than in the healthy individuals (Figure 1D). This suggests that survivors of natural SARS-CoV-2 infection mount a protective immune response related to GCs, which may sustain long-term immunity.

SARS-CoV-2 Seroconversion in Macaques

Following primary SARS-CoV-2 infection of the macaques, seroconversion was measured based on the levels of circulating plasma IgM, IgG, and IgA that bind to S1 and S2 of SARS-CoV-2 (Figure 2A). A significant increase in the levels of antigen-specific IgM was observed 7 days postinfection (dpi) and peaked at 7 or 14 dpi (2-fold) (Figure 2B and Supplementary Figure 1). A significant increase in switched immunoglobulins, including IgG and IgA (2.5- and 4.5-fold) was noted, which peaked at 14 dpi (Figure 2B and Supplementary Figure 1), suggesting immunoglobulin seroconversion. NA was measured at 3 and 21 dpi; consistent with the antibody titers, viral infectivity was reduced by 50% at 3 dpi and decreased up to 21 dpi (Figure 2C).

SARS-CoV-2 Infection-Induced GC Formation

We investigated the relationship between protective antibody production and GC formation in various lymphoid tissues. The frequencies of GC B cells ($IgD^{-}Ki67^{+}CD20^{+}$) (Figure 3A and 3B) and

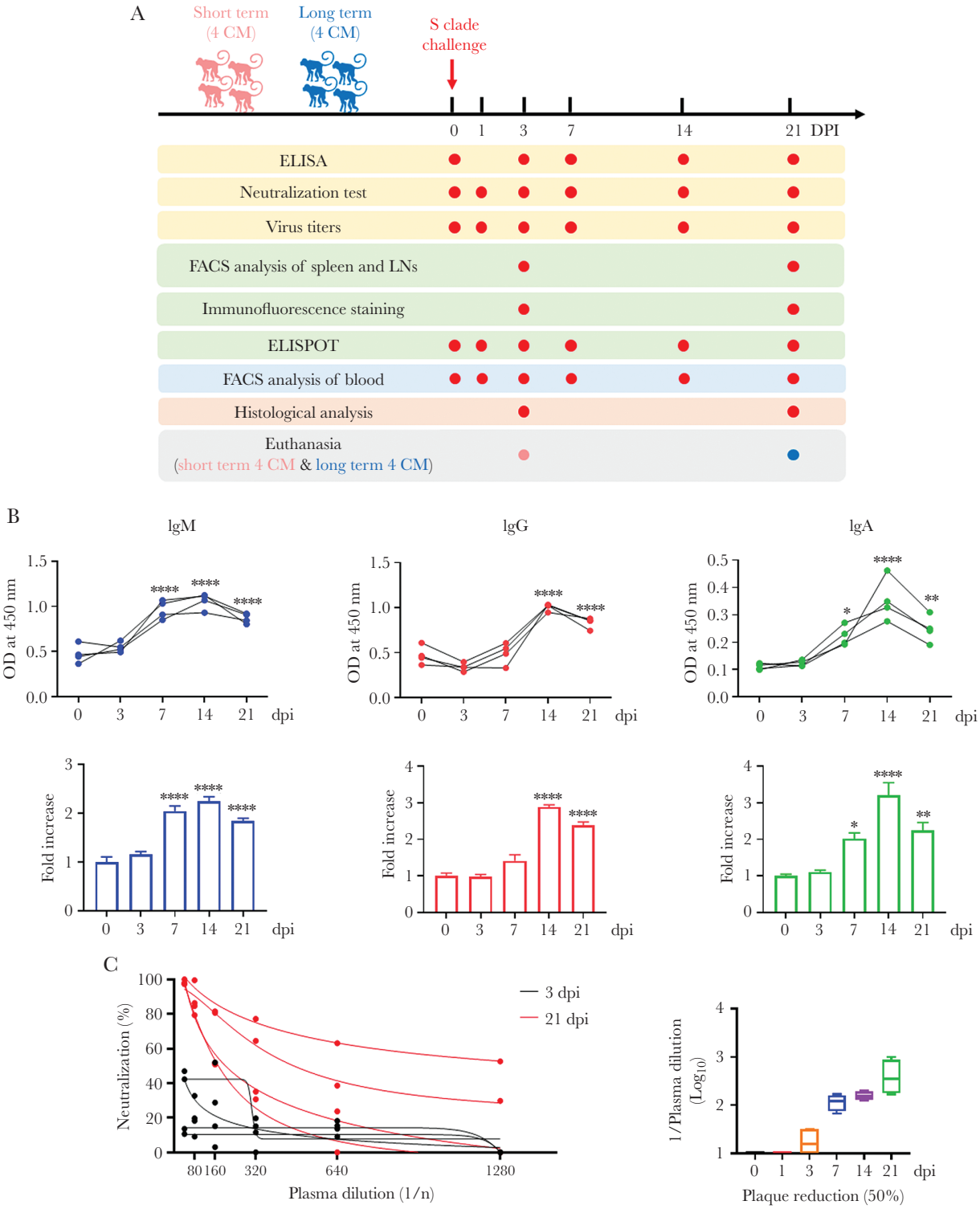

Figure 2. SARS-CoV-2 seroconversion in macaques. *A*, Study design. *B*, IgM, IgG, and IgA antibody responses specific for SARS-CoV-2 spike protein (S1+S2) in plasma collected at 0, 3, 7, 14, and 21 dpi measured using ELISA. Fold change in IgM, IgG, and IgA antibody responses determined by dividing with the values measured at 0 dpi (1-way analysis of variance with Dunnett test for multiple comparisons vs 0 dpi; $*P < .05$, $**P < .01$, $****P < .0001$). Data are presented as mean ± SEM. *C*, Neutralization was determined according to the plasma dilution at the indicated dpi. The SARS-CoV-2 plaque reduction was 50%. Abbreviations: CM, cynomolgus macaque; dpi, days postinfection; ELISA, enzyme-linked immunosorbent assay; ELISPOT, enzyme-linked immunospot; FACS, fluorescence-activated cell sorting; Ig, immunoglobulin; LN, lymph node; OD, optical density; SARS-CoV-2, severe acute respiratory syndrome coronavirus 2.

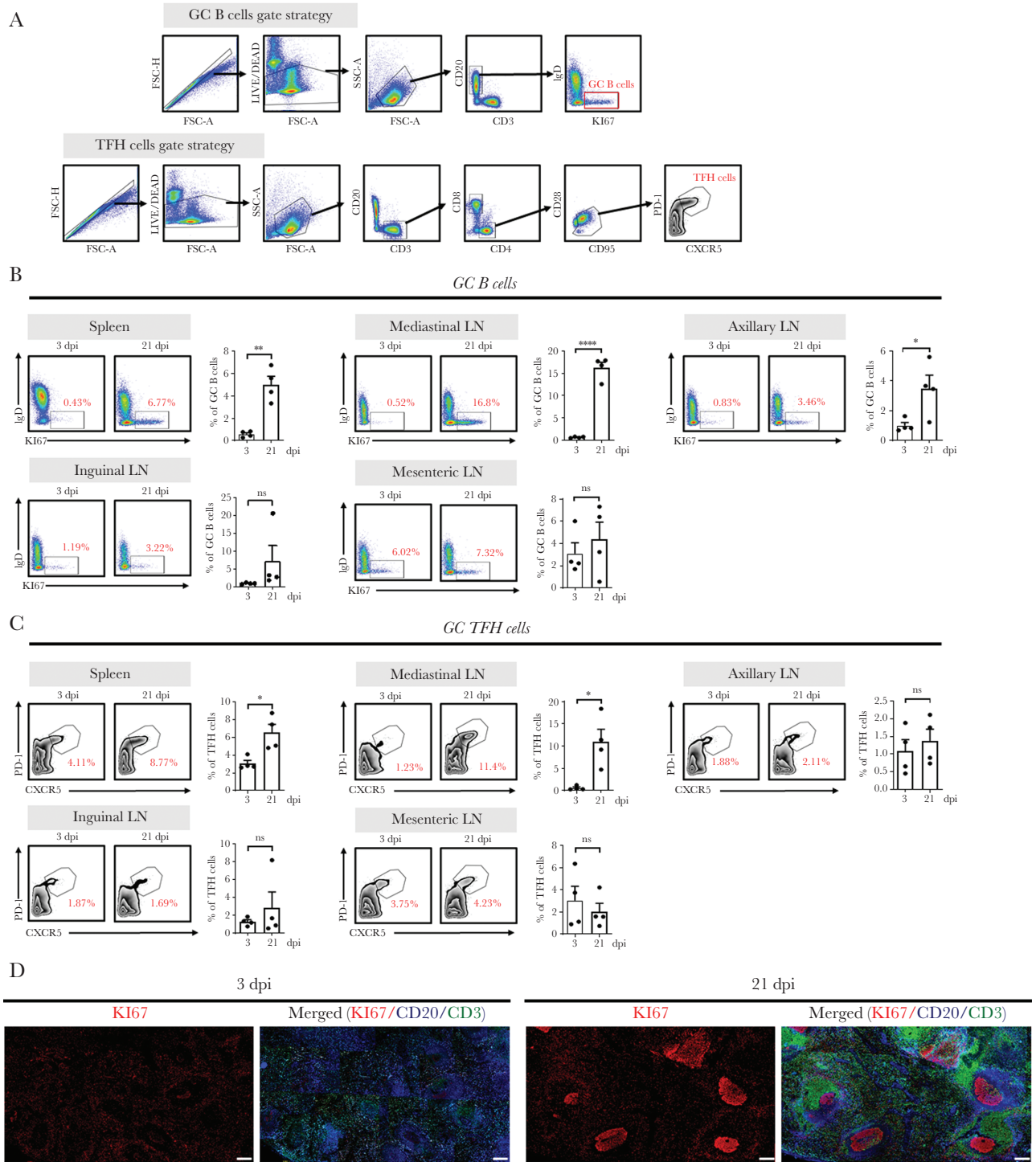

Figure 3. SARS-CoV-2 infection induces GC formation. *A*, Representative gating strategy for GC B and TFH cells. *B*, Frequency of GC B cells in the spleen, LN, axillary LN, inguinal LN, and mesenteric LN collected at 3 and 21 dpi. Data are presented as mean ± SEM (unpaired Student *t* test; **P* < .05, ***P* < .01, *****P* < .0001). *C*, Frequency of TFH cells in the spleen, mediastinal LN, axillary LN, inguinal LN, and mesenteric LN at 3 and 21 dpi (unpaired Student *t* test; **P* < .05). Circles represent individual data obtained from a macaque and bar represents mean ± SEM. *D*, Representative multicolor immunofluorescence images of CD20 (blue), Ki67 (red), and CD3 (green) staining in the spleens at 3 and 21 dpi. Scale bar = 200 μm. Abbreviations: dpi, days postinfection; FSC, forward scatter; GC, germinal center; IgD, immunoglobulin D; LN, lymph node; ns, not significant; PD-1, programmed cell death protein 1; SARS-CoV-2, severe acute respiratory syndrome coronavirus 2; SEM, standard error of the mean; SSC, side scatter; TFH, T follicular helper.

GC TFH cells (PD-1^{high}CXCR5^{+}CD3^{+}CD4^{+}) (Figure 3A and 3C) were significantly higher in the spleen and mediastinal LNs after seroconversion than those before seroconversion; this was confirmed through immunohistochemistry (Supplementary Figure 2). There was a significant increase in mediastinal LNs around the lower respiratory tract at 21 dpi compared with that at 3 dpi (Figure 3B and

3C), coinciding with the reported location of viral replication [11]. B cells ($Ki67^{+}CD20^{+}$) exhibited robust proliferation within follicles at 21 dpi compared with that at 3 dpi (Figure 3D), suggesting GC formation following primary SARS-CoV-2 infection.

ASCs in Lymphoid Tissues and Blood

ASCs generated in lymphoid tissues and blood, following GC formation, may produce antibodies against SARS-CoV-2. To investigate whether ASC generation depends on GC formation, the number of S1 and S2-specific ASCs was measured pre- and postseroconversion. In the spleen, IgM-secreting cells were detectable at 3 dpi, but their numbers sharply decreased at 21 dpi (Figure 4A), suggesting an early GC event before seroconversion. In contrast, IgG-secreting cells were undetectable at 3 dpi, but significantly increased at 21 dpi (Figure 4A), suggesting a late GC event postseroconversion. In the blood, IgM-secreting

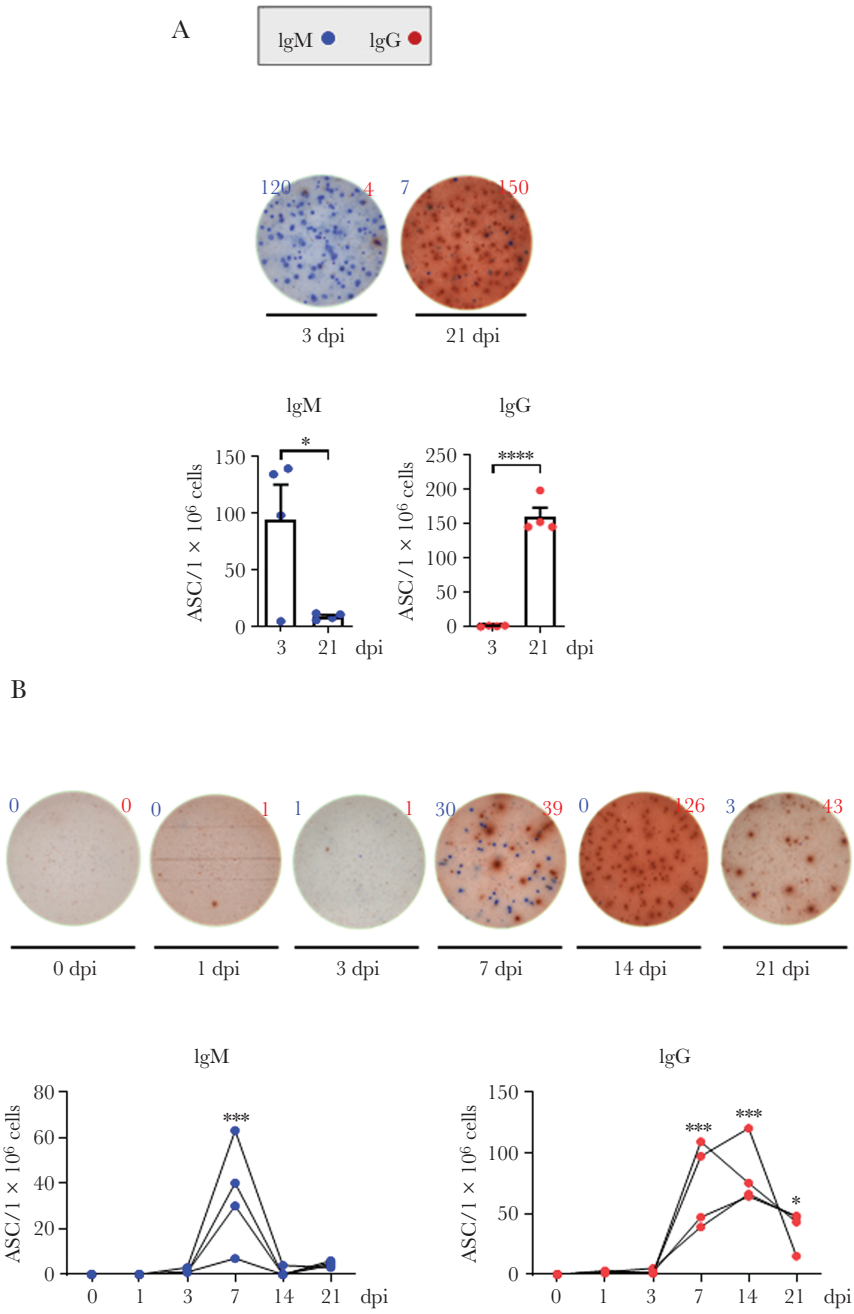

Figure 4. ASCs in lymphoid tissues and blood. *A*, SARS-CoV-2 spike protein (S1+S2)-specific IgM (blue) and IgG (red) ASCs were quantified in the spleen (n = 4) at 3 and 21 dpi using an ELISPOT assay. Circles represent individual data obtained from each macaque and bars represent mean ± SEM (unpaired Student *t* test; $*P < .05$, $****P < .0001$). *B*, The ASCs were enumerated in peripheral blood mononuclear cells (n = 4) at the indicated dpi (1-way analysis of variance with Dunnett test for multiple comparisons vs 0 dpi; $*P < .05$, $***P < .001$). Abbreviations: ASC, antibody-secreting cell; dpi, days postinfection; ELISPOT, enzyme-linked immunospot; Ig, immunoglobulin; SARS-CoV-2, severe acute respiratory syndrome coronavirus 2; SEM, standard error of the mean.

cells increased at 7 dpi, but rapidly declined to baseline. In contrast, the number of IgG-secreting cells began to increase at 7 dpi and continued to increase up to 14 dpi, before decreasing (Figure 4B). Antibody-secreting effector cells were clearly present in the blood, but not as consistently as in the lymphoid tissues.

MBCs in Lymphoid Tissues and Blood

MBCs generated in GCs may help maintain long-term serologic memory. Following SARS-CoV-2 infection, the frequency or absolute number of MBCs ($CD20^+CD3^-IgD^-IgG^+$) significantly increased in the blood and lymphoid tissues postseroconversion (Figure 5A and 5B). This suggests that the GC-dependent MBC generation detected in the blood is related to the production of protective antibodies. However, surface marker-based identification helps detect the entire MBC population, not just those from SARS-CoV-2 infection; therefore, we examined the quantity and quality of MBCs specific for SARS-CoV-2. For MBCs to differentiate into

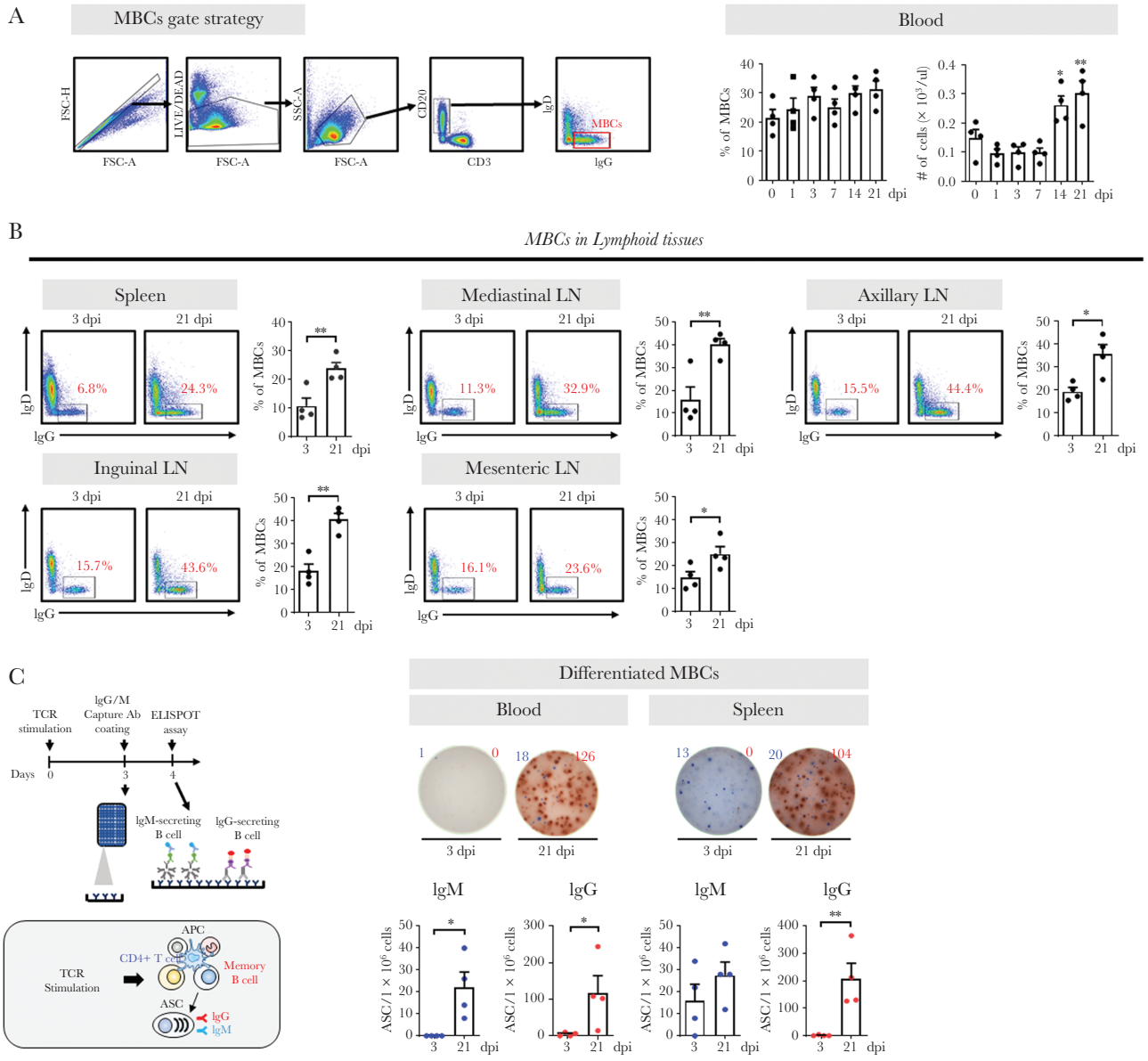

Figure 5. MBCs in lymphoid tissues and blood. *A*, Representative gating strategy for MBCs. Frequency and absolute numbers of MBCs in the blood (1-way analysis of variance with Dunnett test for multiple comparisons vs 0 dpi; $*P < .05$, $**P < .01$). *B*, Frequency of MBCs in the spleen, mediastinal LN, axillary LN, inguinal LN, and mesenteric LN at 3 and 21 dpi (unpaired Student *t* test; $*P < .05$, $**P < .01$). Circles represent individual data obtained from each macaque and bars represent mean ± SEM. *C*, Schematic diagram of the ELISPOT assay after TCR stimulation. SARS-CoV-2 spike protein (S1+S2)-specific IgM (blue) and IgG (red) ASCs were enumerated in MBCs activated by anti-CD3 and anti-CD28 monoclonal antibodies (1 μg/mL) in peripheral blood mononuclear cells (n = 4) and the spleen (n = 4) after 4-day culture. The ASCs were determined using the ELISPOT assay and are shown as mean ± SEM (unpaired Student *t* test; $*P < .05$, $**P < .01$). Abbreviations: Ab, antibody; APC, antigen-presenting cell; ASC, antibody-secreting cell; dpi, days postinfection; ELISPOT, enzyme-linked immunospot; Ig, immunoglobulin; LN, lymph node; MBC, memory B cell; SARS-CoV-2, severe acute respiratory syndrome coronavirus 2; SEM, standard error of the mean; TCR, T-cell receptor.

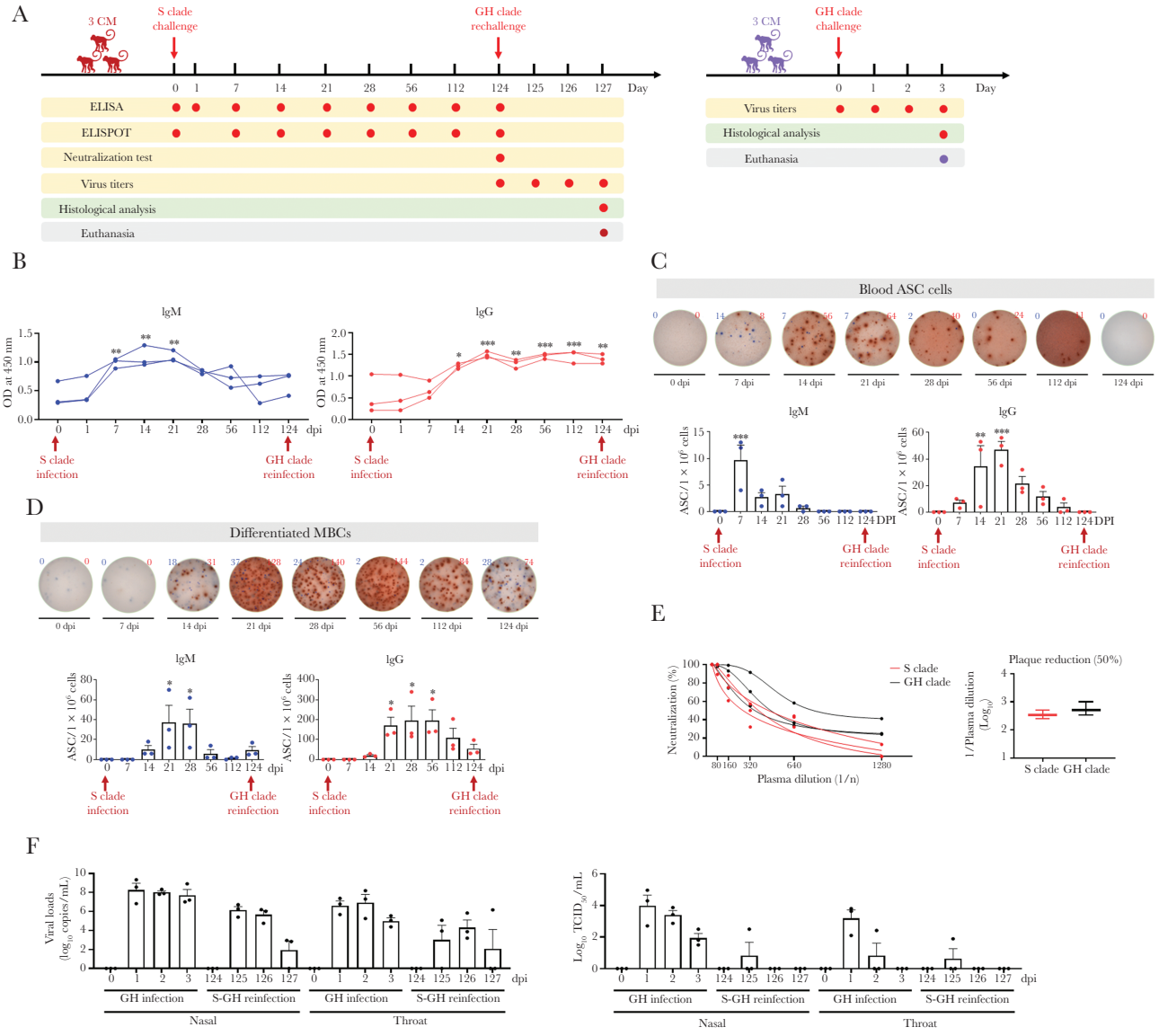

Figure 6. Germinal center-induced cross-protective immunity. *A*, Experimental design. Three macaques were challenged with 12.5 mL of SARS-CoV-2 virus (2.1×10^6 $TCID_{50}$/mL, S clade). After the ASCs from the primary infection had disappeared from all infected macaques, 3 infected macaques were rechallenged at 124 dpi with the SARS-CoV-2 GH clade. Additionally, 3 uninfected monkeys (controls) were challenged at 0 dpi with the same SARS-CoV-2 (GH clade) as that used to reinfect animals. *B*, IgM and IgG antibody responses specific for SARS-CoV-2 spike (S1+S2) proteins were analyzed using plasma collected at 0, 1, 7, 14, 21, 28, 56, 112, and 124 dpi following the initial infection, using the ELISA (1-way ANOVA with Dunnett test for multiple comparisons vs 0 dpi; $*P < .05$, $**P < .01$, $***P < .001$). *C*, Representative ELISPOT data of SARS-CoV-2 spike protein (S1+S2)-specific IgM (blue) and IgG (red) ASCs in peripheral blood mononuclear cells of primary-challenged primates. Circles represent individual data (1-way ANOVA with Dunnett test for multiple comparisons vs 0 dpi; $**P < .01$, $***P < .001$). *D*, Representative ELISPOT data of SARS-CoV-2 spike protein (S1+S2)-specific IgM (blue) and IgG (red)-secreting cells differentiated from MBCs over 4 days using anti-CD3 and anti-CD28 monoclonal antibodies (1 μg/mL). Circles represent individual data (1-way ANOVA with Dunnett test for multiple comparisons vs 0 dpi; $*P < .05$). *E*, After infection with the S and GH clade, neutralization indicated according to plasma dilution at 124 dpi. *F*, Virus titers of swab samples in which viral RNA (copies/mL) was quantified using qRT-PCR and $TCID_{50}$/mL was determined. Circles represent individual data and bar values represent mean ± SEM. Abbreviations: ANOVA, analysis of variance; ASC, antibody-secreting cell; CM, cynomolgus macaque; dpi, days postinfection; ELISA, enzyme-linked immunosorbent assay; ELISPOT, enzyme-linked immunospot; Ig, immunoglobulin; MBC, memory B cell; OD, optical density; qRT-PCR, quantitative reverse transcription polymerase chain reaction; SARS-CoV-2, severe acute respiratory syndrome coronavirus 2; $TCID_{50}$, 50% tissue culture infectious dose.

ASCs producing SARS-CoV-2–specific antibodies, helper CD4 T cells are required along with antigen-presenting cells (Figure 5C). These cell-cell interactions are similar to those observed between TFH-follicular dendritic cells and GC B cells in the light zone of GCs [2, 16]. ASCs were generated by stimulating T-cell receptors with CD3 and CD28 antibodies (Supplementary Figure 3A). This was mediated by CD4 T cells, and not CD8 T cells; it occurred only in the presence of memory CD4 T cells and was not limited to circulating CD4 T cells with CXCR5 expression (Supplementary Figure 3B and 3C). The reaction was limited to MBCs, not naive B cells, and was further amplified by antigen-presenting cells

(Supplementary Figure 3D and 3E). High levels of IgG-secreting cells differentiated from MBCs were detected in the blood and spleen of all animals at 21 dpi but were undetectable at 3 dpi (Figure 5C).

GC-Induced Cross-Protective Immunity

To understand whether SARS-CoV-2–specific GC activity, elicited following the initial infection, imparted protection against reinfection with SARS-CoV-2 variants, we rechallenged 3 adult cynomolgus macaques with the GH clade on day 121 postrecovery from primary SARS-CoV-2 infection with the S clade (Figure 6A). Three naive animals were used as the positive controls. After seroconversion, the circulating IgGs specific for the S protein, receptor binding domain, and nucleocapsid protein persisted at 124 dpi before the rechallenge (Figure 6B and Supplementary Figure 4), whereas the number of GC cells including ASCs and MBCs declined (Figure 6C and 6D). Consistent with the antibody titers, infected animals exhibited NA against live SARS-CoV-2 virus (S clade and GH clade) (Figure 6E), suggesting the presence of SARS-CoV-2–specific GC activity before rechallenge. During rechallenge, the recovered animals showed no significant increase in body temperature and the lymphocytes decreased but to a lesser extent than in the positive controls (Supplementary Figure 5). The infectious virus was undetectable in nasal and oral swabs 2 days after reinfection and in the lung 3 days after reinfection (Figure 6F and Supplementary Figure 6). Additionally, the RT-PCR results revealed low and median viral loads in nasal and throat swabs during the rechallenge and in each lobe of the lungs at 3 dpi (Figure 6F and Supplementary Figure 6). This suggests that long-term immunity, including GC activity, in survivors of natural SARS-CoV-2 infection effectively controls viral replication during subsequent infection.

Lung Damage During Reinfection

We evaluated histopathologic lung sections. Consistent with acute interstitial pneumonia in macaques at 3 dpi

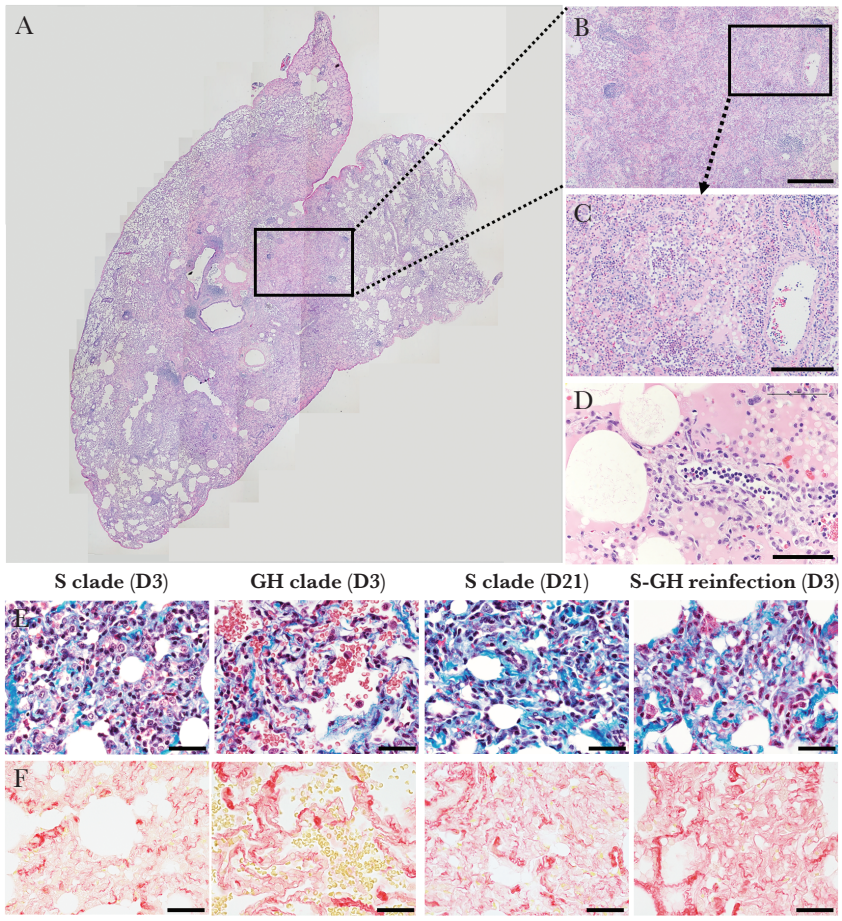

Figure 7. Lung damage during reinfection. *A*, Low magnification merged image of a hematoxylin and eosin-stained section of the lower lung lobe of a macaque at 3 days after reinfection. *B*, Alveolar septa and lumina infiltrated by immune cells, accompanied by alveolar filling with eosinophilic edema and fibrin. Scale bar = 400 μm. *C*, Loss of alveolar wall structure caused by edema and pneumocyte necrosis. Substantial migration of neutrophils observed in alveolar lumina and around blood vessels. Scale bar = 200 μm. *D*, Hyaline membranes deposited along the injured alveolar walls. Scale bar = 100 μm. *E* and *F*, The lung lobes of macaques infected with the S clade or GH clade or sequentially infected macaques (S clade and GH clade) stained with Masson's trichrome (*E*) and Sirius red (*F*). Blue in Masson's trichrome staining (*E*) and red in Sirius red staining (*F*) indicate collagen deposition. Scale bar = 40 μm.

(Supplementary Figure 7A–7D), as described previously [11, 13], the main histological lesions consisted of areas with acute diffuse alveolar damage (Figure 7A–7D). In these areas, the lumina of alveoli were variably filled with neutrophils, macrophages, and a few lymphocytes. Mononuclear cells and neutrophils had also infiltrated the wall. One sample showed severe migration of neutrophils in the alveolar lumen, wall, and around blood vessels (Figure 7B and 7C); hyaline membranes were observed in a few damaged alveoli (Figure 7D). Neutrophils and mononuclear leukocytes attached to the endothelium of blood vessels, indicating the degeneration of endothelial cells. Aggregates of neutrophils and mononuclear leukocytes were observed around pulmonary vessels with endothelial changes (Figure 7D). In the lesions, except those with severe pulmonary edema, the alveolar walls had moderately thickened due to type II pneumocyte hyperplasia and infiltration of neutrophils and mononuclear leukocytes, without edema in the alveolar lumina. Consistent with these pathological observations, the severity score of lesions was higher in rechallenged macaques than in those at 21 dpi (Supplementary Figure 7E). Additionally, collagen deposits, which may lead to irreversible lung damage with architectural distortion, were detected extensively in the alveolar septae and around the vessels of rechallenged animals, similar to those seen in macaques at 21 dpi (Figure 7E and 7F). Therefore, SARS-CoV-2 rechallenge induces diffuse alveolar damage in the lungs combined with increased fibrotic tissue.

DISCUSSION

GC activity in secondary lymphoid tissues is essential for the generation of most isotype-switched and affinity-matured antibodies with NA and long-lasting B-cell memory. Herein, we described the kinetics of GC-related cells, including ASCs and MBCs, in the lymphoid tissues and blood during SARS-CoV-2 infection, allowing the evaluation of protective humoral immune responses. In COVID-19 survivors, it is difficult to accurately determine the exact time of seroconversion after natural pathogen exposure and the corresponding changes in GC activity in the lymphoid tissues. Therefore, macaques, which recapitulate COVID-19 with mild or moderate symptoms in humans [11–13], were used here.

Immunoglobulins, including neutralizing antibodies elicited by human coronaviruses, are correlated with immunity at symptom onset [17]; there is a strong correlation between switched immunoglobulin titers and neutralizing antibodies in circulation [8, 18]. Our data show that SARS-CoV-2–specific MBCs were evident in convalescent patients with a high level of switched immunoglobulins and protective antibodies in circulation. There was also a clear increase in size and/or activity of GCs in lymphoid tissues and blood postseroconversion in macaques infected with SARS-CoV-2. These results suggest that seroconversion with protective antibody production is dependent on GC activity-mediated immunoglobulin switching during primary SARS-CoV-2 infection. It is likely that GC-related immune responses are correlated with protection against reexposure to a homogeneous virus. Protective antibodies isolated from convalescent patients provide protection against disease in SARS-CoV-2–infected mice, hamsters, and rhesus macaques [19–21]. Additionally, SARS-CoV-2–infected rhesus macaques display a robust antibody response upon reexposure soon after the primary infection [22, 23]. Here, all animals that recovered from the SARS-CoV-2 S clade infection displayed the definite GC response specific for virus and showed notable decline in replicating virus titers and viral RNA when reexposed to the GH clade 4 months after the primary infection. Before the rechallenge, GC-related immune responses were evidently directed at neutralizing both S and GH clades, indicating that the virus-specific GC activity may be a promising biomarker for virus control after reexposure to SARS-CoV-2. However, SARS-CoV-2 rechallenge in the recovered macaques was associated with diffuse alveolar damage along with collagen deposition in the lungs. GC-related immunity against reexposure to SARS-CoV-2 variants may be helpful for early control of viral replication but may not necessarily prevent lung damage when viruses reach the lower respiratory tract. Therefore, studies on lung pathogenesis upon reinfection in humans are vital to assess pulmonary impact and COVID-19 management.

To determine the dynamic activity of GCs during viral infection, we examined TFH cells and GC B cells, which are required for GC development, somatic hypermutation, and affinity maturation [2]. We observed a significant increase in TFH and B cells in lymphoid tissues after seroconversion, following primary SARS-CoV-2–infection in macaques. However, this is only indirect evidence and does not indicate the specificity of these cells for SARS-CoV-2 antigens. Therefore, GC cells, including MBCs and ASCs, specific for SARS-CoV-2 antigens were examined. In macaque LN tissue infected with SARS-CoV-2, viral antigen-specific IgM-secreting cells and IgM MBCs were clearly observed at 3 dpi; however, after seroconversion, the number of IgM-secreting cells declined in the LNs, whereas that of MBCs increased. SARS-CoV-2–specific IgG-secreting cells and IgG MBCs were evident only after seroconversion, suggesting that immunoglobulin switching occurred after the GC late events. The viral titer is low or undetectable in the upper airways and lungs prior to seroconversion [11], and further studies are essential to determine the role of antigen-specific IgM in the protective humoral immune response that controls SARS-CoV-2 spread in the early stages of primary infection. In SARS-CoV-2–specific ASCs in the blood, IgM was not detectable after 7 dpi, whereas IgG increased from 7 dpi to 14 dpi, and then decreased. However, the number and frequency of viral antigen-specific MBCs increased significantly postseroconversion and remained high until 21 dpi. The level of MBCs may be more consistent than that of ASCs, and thus MBCs may serve as a stable blood biomarker for GC development.

GCs can provide protection against reinfection; however, there remains a concern that SARS-CoV-2 may stimulate MBC generation and therefore decrease antibody production. Thus, if antibodies are not detectable, it is necessary to determine whether they disappeared due to MBC generation following a decrease in viral antigen or whether the generation of MBCs is poor owing to the absence of GCs due to symptom severity. Virus-specific antibodies against SARS-CoV-2 were detected in 100% of the patients in this study within 19 days after symptom onset [7]; circulating IgM and IgG were produced, and they persisted even after the patients stopped shedding the virus, probably resulting in negative RT-PCR results [6]. Serological tests based on circulating antibodies indicate that COVID-19 prevalence is low despite the great impact of the pandemic in many countries [5, 24, 25]. Additionally, the level of virus-specific antibodies, including neutralizing antibodies, decreases to undetectable levels in convalescent patients after 2–3 months [4, 5, 26], suggesting impaired humoral immunity in these patients. It is possible that circulating immunoglobulins disappeared from the peripheral blood at some point after seroconversion. Therefore, simultaneous measurement of circulating antibodies and memory cells is useful in determining whether seroconversion occurs in patients with COVID-19, or antibody counts simply decrease during the infection.

Antibody deficiency may contribute to disease severity; however, there is currently no direct evidence that SARS-CoV-2 infection lacks a repertoire of immune memory cells. Low levels of somatic hypermutation and plasma NAs are observed in convalescent patients with COVID-19 [27, 28] suggesting that SARS-CoV-2 can affect immune memory quality. The decline in immune memory quality could be because of the disruption of GCs in lymphoid tissues. Poor GC formation and GC cell loss, such as TFH cells and B cells, in secondary lymphoid follicles has been reported in patients with fatal COVID-19 [10]; however, this is confined to severely ill patients and it cannot explain the role of GCs in the host defense in most convalescent COVID-19 cases.

Our data demonstrated that a robust GC response was positively correlated with a protective immune response in COVID-19 patients with less severe disease. It is not surprising that the GC response is indispensable for virus elimination, and poor GC formation, without evidence of seroconversion, is correlated with rapid disease progression and higher mortality, similar to human immunodeficiency virus/simian immunodeficiency virus (HIV/SIV) infection [15, 29]. Therefore, GC-related immune memory responses acquired through recovery from SARS-CoV-2 infection influence recovery from COVID-19. However, when the disease becomes more serious, cytokines such as tumor necrosis factor (TNF) have a deleterious effect on the formation of memory cells [10], which may interfere with protection against reinfection. Therefore, GC activity may be predictive of disease progression to severe stages and is important in protection against reinfection with SARS-CoV-2. Measuring GC-associated memory can be a useful tool for predicting protection against future infection. Nevertheless, this study had some limitations. First, we did not provide long-term evidence in humans or macaques on whether the virus can slowly neutralize GCs during natural primary SARS-CoV-2 infection. Second, LN tissues from human patients recovered from the infection were not analyzed here.

In conclusion, the seroconversion observed in macaques, which recapitulates the course of COVID-19 disease in human survivors with mild or moderate symptoms, was consistent with the response of GCs in lymphoid tissues and blood of the human subjects tested. Circulating antibodies and MBCs specific to SARS-CoV-2 were more consistently present than ASCs and, therefore, they can be used to predict GC-related protective humoral immune responses. Convalescent patients with COVID-19 also showed similar anti-SARS-CoV-2–specific B-cell responses related to GC activity, which might protect against reinfection. The GC activity in macaques that recovered from SARS-CoV-2 primary infection protects against rechallenge with a different clade of virus; however, rechallenge led to lung damage along with collagen deposition in the recovered macaques. In most human survivors with mild-to-moderate COVID-19, the presence of GCs and the production of neutralizing antibodies specific for SARS-CoV-2 may potentially control the virus. Nevertheless, alleviation of diffuse alveolar damage and fibrotic tissues induced by SARS-CoV-2 reexposure warrants further investigation.

Supplementary Data

Supplementary materials are available at *The Journal of Infectious Diseases* online. Consisting of data provided by the authors to benefit the reader, the posted materials are not copyedited and are the sole responsibility of the authors, so questions or comments should be addressed to the corresponding author.

Notes

Acknowledgment. The authors thank the staff of the Korea National Primate Research Centre for their excellent veterinary care.

Author contributions. G. K., S. K., D. H. K., H. O., J. P., and J. J. H. analyzed the data and wrote the manuscript. G. K., B. K., H. O., E. H., H. J., Y. J. A., S. H. B., M. K., J. K., P. K., S. B., E. L., and J. J. H. performed the experiments and managed the animals. D. H. K., S. K., J. P., K. L., and C. R. provided scientific input. J. J. H. was responsible for the conceptualization and design of the study.

Financial support. This work was supported by the Ministry of Science and Information and Communications Technologies of Korea (grant number PRM1752011); Korea Research Institute of Bioscience and Biotechnology Research Initiative

Programs (grant number KGM 4572013); and the Korea Centers for Disease Control and Prevention (grant number 2020-ER5321-00).

Potential conflicts of interest. All authors: No reported conflicts of interest. All authors have submitted the ICMJE Form for Disclosure of Potential Conflicts of Interest. Conflicts that the editors consider relevant to the content of the manuscript have been disclosed.

References

1. De Silva NS, Klein U. Dynamics of B cells in germinal centres. Nat Rev Immunol **2015**; 15:137–48.
2. Crotty S. T follicular helper cell differentiation, function, and roles in disease. Immunity **2014**; 41:529–42.
3. Baumgarth N. How specific is too specific? B-cell responses to viral infections reveal the importance of breadth over depth. Immunol Rev **2013**; 255:82–94.
4. Long QX, Tang XJ, Shi QL, et al. Clinical and immunological assessment of asymptomatic SARS-CoV-2 infections. Nat Med **2020**; 26:1200–4.
5. Pollán M, Pérez-Gómez B, Pastor-Barriuso R, et al; ENE-COVID Study Group. Prevalence of SARS-CoV-2 in Spain (ENE-COVID): a nationwide, population-based seroepidemiological study. Lancet **2020**; 396:535–44.
6. Guo L, Ren L, Yang S, et al. Profiling early humoral response to diagnose novel coronavirus disease (COVID-19). Clin Infect Dis **2020**; 71:778–85.
7. Long QX, Liu BZ, Deng HJ, et al. Antibody responses to SARS-CoV-2 in patients with COVID-19. Nat Med **2020**; 26:845–8.
8. Amanat F, Stadlbauer D, Strohmeier S, et al. A serological assay to detect SARS-CoV-2 seroconversion in humans. Nat Med **2020**; 26:1033–6.
9. Ju B, Zhang Q, Ge J, et al. Human neutralizing antibodies elicited by SARS-CoV-2 infection. Nature **2020**; 584:115–9.
10. Kaneko N, Kuo HH, Boucau J, et al; Massachusetts Consortium on Pathogen Readiness Specimen Working Group. Loss of Bcl-6-expressing T follicular helper cells and germinal centers in COVID-19. Cell **2020**; 183:143–57.e13.
11. Koo BS, Oh H, Kim G, et al. Transient lymphopenia and interstitial pneumonia with endotheliitis in SARS-CoV-2-infected macaques. J Infect Dis **2020**; 222:1596–600.
12. Munster VJ, Feldmann F, Williamson BN, et al. Respiratory disease and virus shedding in rhesus macaques inoculated with SARS-CoV-2. Nature **2020**; 585:268–272.
13. Rockx B, Kuiken T, Herfst S, et al. Comparative pathogenesis of COVID-19, MERS, and SARS in a nonhuman primate model. Science **2020**; 368:1012–5.
14. Hong JJ, Amancha PK, Rogers K, Ansari AA, Villinger F. Re-evaluation of PD-1 expression by T cells as a marker for immune exhaustion during SIV infection. PLoS One **2013**; 8:e60186.
15. Hong JJ, Amancha PK, Rogers KA, et al. Early lymphoid responses and germinal center formation correlate with lower viral load set points and better prognosis of simian immunodeficiency virus infection. J Immunol **2014**; 193:797–806.
16. Victora GD, Nussenzweig MC. Germinal centers. Annu Rev Immunol **2012**; 30:429–57.
17. Huang AT, Garcia-Carreras B, Hitchings MDT, et al. A systematic review of antibody mediated immunity to coronaviruses: kinetics, correlates of protection, and association with severity. Nat Commun **2020**; 11:4704.
18. Okba NMA, Müller MA, Li W, et al. Severe acute respiratory syndrome coronavirus 2-specific antibody responses in coronavirus disease patients. Emerg Infect Dis **2020**; 26:1478–88.
19. Rogers TF, Zhao F, Huang D, et al. Isolation of potent SARS-CoV-2 neutralizing antibodies and protection from disease in a small animal model. Science **2020**; 369:956–63.
20. Shi R, Shan C, Duan X, et al. A human neutralizing antibody targets the receptor-binding site of SARS-CoV-2. Nature **2020**; 584:120–4.
21. Cao Y, Su B, Guo X, et al. Potent neutralizing antibodies against SARS-CoV-2 identified by high-throughput single-cell sequencing of convalescent patients' B cells. Cell **2020**; 182:73–84.e16.
22. Chandrashekar A, Liu J, Martinot AJ, et al. SARS-CoV-2 infection protects against rechallenge in rhesus macaques. Science **2020**; 369:812–7.
23. Deng W, Bao L, Liu J, et al. Primary exposure to SARS-CoV-2 protects against reinfection in rhesus macaques. Science **2020**; 369:818–23.
24. Salje H, Tran Kiem C, Lefrancq N, et al. Estimating the burden of SARS-CoV-2 in France. Science **2020**; 369:208–11.
25. Sood N, Simon P, Ebner P, et al. Seroprevalence of SARS-CoV-2-specific antibodies among adults in Los Angeles County, California, on April 10–11, 2020. JAMA **2020**; 323:2425–7.
26. Seow J, Graham C, Merrick B, et al. Longitudinal observation and decline of neutralizing antibody responses in the three months following SARS-CoV-2 infection in humans. Nat Microbiol **2020**; 5:1598–607.
27. Robbiani DF, Gaebler C, Muecksch F, et al. Convergent antibody responses to SARS-CoV-2 in convalescent individuals. Nature **2020**; 584:437–42.
28. Brouwer PJM, Caniels TG, van der Straten K, et al. Potent neutralizing antibodies from COVID-19 patients define multiple targets of vulnerability. Science **2020**; 369:643–50.
29. Hong JJ, Chang KT, Villinger F. The dynamics of T and B cells in lymph node during chronic HIV infection: TFH and HIV, unhappy dance partners? Front Immunol **2016**; 7:522.